

Supplementary Information

Changing interaction strength between magnetically coupled dimers

Adam Berlie, Ian Terry, Marek Szablewski and Sean Giblin

February 4, 2016

1 X-Ray Diffraction

Powder X-ray diffraction was conducted using a Pananalytical diffractometer where a monochromatic source of Cu-radiation was used. The sample was placed on a silicon plate at room temperature and a spinner was used to provide a better averaging over all crystallites.

The structure of KTCNQF₄ is assumed to be similar to that of KTCNQ [1] with stacking of the TCNQF₄ molecules along the *a*-axis. The sample grows as very fine needles that are a darker purple in colour. At first powder diffraction was conducted on a sample where a Le Bail refinement was performed, the unit cell parameters calculated can be seen in 1.

Unit Cell Parameter	Value
<i>a</i>	3.55 Å
<i>b</i>	12.36 Å
<i>c</i>	12.03 Å
β	95.63°
Volume	525.6 Å ³

Table 1: Unit cell parameters from a LeBail refinement of the powder diffraction pattern for the $P2_1/c$ space group.

The data was refined using the space group $P2_1/c$, which is similar to KTCNQ when it is in the high temperature higher symmetry phase i.e. above the spin-Peierls transition. In order to get a decent fit to the data extra impurity phases had to be introduced; potassium iodide and neutral TCNQ. From the Le Bail refinement this equated to 0.051% and 1.19% respectively. It should be noted that these figures should be taken lightly and are an indication of the amount of impurity phase but not a true representation. One refining the pattern the $R_p = 5.18$ and the $wR_p = 7.70$. Although this is not as low as desirable the sample is very close to the protio sample and shows the same structure in the high-temperature phase. From the refinement the *a* lattice parameter is similar to the protio counterpart, however the other lattice parameters are all lower. This may indicate that on the addition of fluorine to the TCNQ molecule, this is able to cause a stronger interaction between ionic species which in turn causes a shrinking of the unit cell. More analysis is needed of the diffraction patterns in order to fully elucidate the structure and will be presented within another manuscript focusing solely on the structural properties of the sample as this is beyond the scope of this current manuscript.

Single crystal diffraction was also attempted on a sample that was recrystallised in an acetonitrile and diethylether mixture. The diffraction data was collected at 150 K and the unit cell was indexed as monoclinic with the space group $P2_1/c$, the same space group for the high temperature phase of KTCNQ, the unit cell parameters were similar as to what was calculated for the powder diffraction data. For the single crystal diffraction data the lattice parameters are similar to the KTCNQ data collected by Konno and Saito [1] except for the *b*-axis which is approximately 0.7 Å shorter. Interestingly at 150 K the continuous magnetic

transition is within the critical region however the structure does not appear to have responded to the Peierls transition and we do not see a doubling of the unit cell. The crystal was tilted to look for extra diffraction spots along the a -axis to see whether there was a doubling of the lattice parameter however nothing was observed. The data were poor due to sample quality and so more work is ongoing to grow a good single crystal for structure refinement.

2 Magnetic Susceptibility

2.1 KTCNQ-H₄

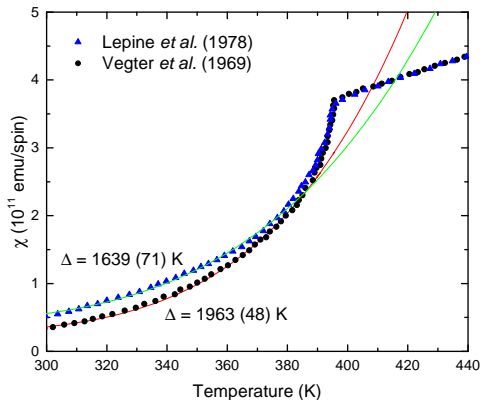


Figure 1: Magnetic susceptibility measurements made previously by Lépine *et al* [2]. and Vegter *et al* [3]. The solid lines are fits of an activated type behaviour as discussed within the main body of the manuscript to give values of the spin gap.

The magnetic susceptibility of KTCNQ has been measured previously by Lépine *et al* [2]. and Vegter *et al* [3]. Data from the manuscripts were digitised using the Origin plotting program to allow a fit to the data in the form of

$$\chi = A_{SP} \exp\left(\frac{-2\Delta}{k_B T}\right) + \chi_0, \quad (1)$$

where A_{SP} is the amplitude, Δ is the energy gap and χ_0 is the baseline that accounts for a non-zero susceptibility at low temperatures. In both cases, the diamagnetic susceptibility was reported to have been corrected for. The fitting parameters have been tabulated below.

Data Set	A_{SP} (emu/spin)	Δ (K)	χ_0 (emu/spin)
Lépine	54000(13000)	1964 (48)	0.25(2)
Vegter	9500(3400)	1639 (71)	0.38(3)

Table 2: Table showing the fitting parameters from Figure 1 to Equation 1.

2.2 KTCNQ-F₄

The magnetic data for KTCNQF₄ is shown in the inset of figure 2 where the Field Cooled (FC) data were collected in an applied field of 5 T. This high field causes the paramagnetic and diamagnetic components to

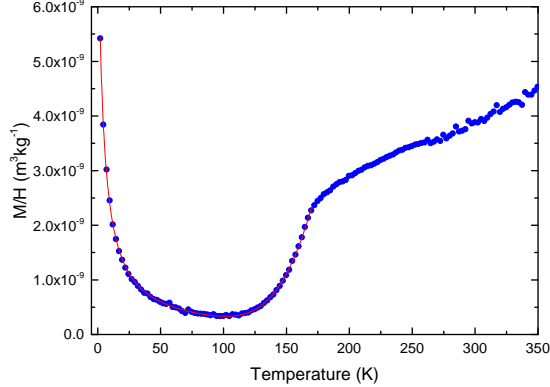


Figure 2: FC M/H of KTCNQF₄ taken in an applied field of 5 T, the solid line shows a fit to the whole data set below T_{SP}^X so the diamagnetic and Curie-Weiss contributions could be subtracted and used to create a more appropriate plot as shown in the main manuscript.

be relatively large. However the whole data set below the transition temperature could be fitted using the equation

$$\chi = A_{SP} \exp\left(\frac{-2\Delta}{k_B T}\right) + \frac{C}{(T - \theta)} + \chi_D. \quad (2)$$

The fit can be seen in Figure 2. The diamagnetic component was calculated to be $-2.0774(6) \times 10^{-8} \text{ m}^3\text{kg}^{-1}$ which is similar to a value obtained from a 0.1 T FC curve from previous results[4], however using values from Pascal's constants one obtains a value of $-1.9 \times 10^{-9} \text{ m}^3\text{kg}^{-1}$ and so, in either case, this may not be a true representation of χ_D as both methods have significant issues (the susceptibility data does not show a clear flat area to estimate χ_D and using Pascal constants involves a crude calculation that uses a summation of diamagnetic susceptibilities of individual atoms and bonds). The Curie-Weiss term accounted for the low temperature behaviour where $C = 3.23(2) \times 10^{-8} \text{ m}^3\text{Kkg}^{-1}$ and $\theta = -3.94(4) \text{ K}$. The Weiss constant, θ , was needed to correct for the curvature at low temperatures and indicates weak antiferromagnetic (AF) interactions between the paramagnetic centres, possibly uncompensated TCNQF₄ radicals states. From the value of C , the mass percentage of paramagnetic defects was calculated to be 0.22% assuming spin only $S = 1/2$ moments.

3 Muon Spectroscopy

Shown are the raw data or spectra at selected temperatures for both the KTCNQ-H₄ and KTCNQ-F₄ samples however the analysis of the temperature outside the SP region is complex and would require more discussion which is outside the scope of work [4]. The background was measured by using a haematite sample and applying a transverse field of 100 G the resulting 4.5% asymmetry was due to the muons relaxing in the sample holder/cryostat and makes up the background of the measurement

At low temperatures ($T < 300 \text{ K}$) the relaxation, as stated, is complex and there may be two present, one at short times outside of the experimental time scale and another within the muon decay time window. However to parametrise the data, the entire temperature dependent spectra were fit with a single exponential, where the results can be seen in figure 5. There appears to be a strong correlation between the asymmetry, where below 150 K there is a significant missing fraction in the asymmetry. The rise in λ may be due to the unfreezing of the quasi-static state where magnetic fluctuations enter the muon time scale. Below the cusp, the fluctuations are frozen out and so the muon relaxation drops and another process dominates. The

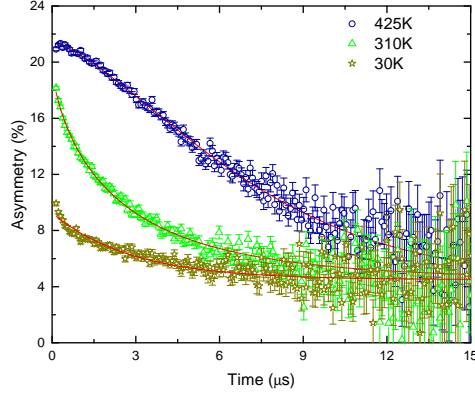


Figure 3: Zero field μ SR raw data for KTCNQ-H₄.

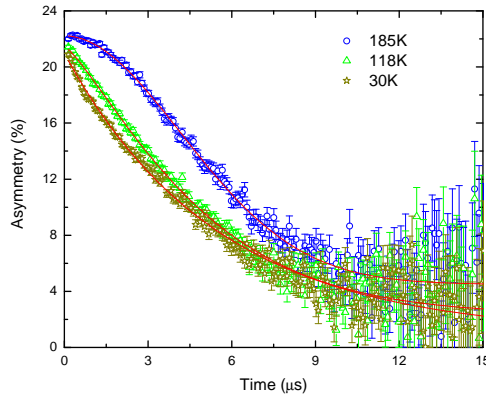


Figure 4: Zero field μ SR raw data for KTCNQ-F₄.

missing fraction below T_{SP} may be suggestive of a significant muonium fraction but within neutral TCNQ Pratt *et al.* observed bonding to the nitrogen [5] with the formation of a radical although this may differ with the anion. If there was a small amount of KI impurity, then this would also lead to a muonium fraction where a significant missing fraction would be observed [6, 7]. Although more likely is the muon implanting in a site with strong internal fields which dephase the muon outside of the time scale, one such site may be between two TCNQ molecules within a dimer where there is significant π -electron density, it should be noted that the internal field that the muon observes does not have to be polarised on a macroscopic scale.

For the KTCNQ-F₄ sample, at low temperatures, the stretched exponential could no longer describe the data as there appeared to be a superposition of a fast and slow relaxation. Instead, these temperatures were analysed using a summation of two exponential relaxations (see figure 6). At 90 K the values of λ increase as the muon is sensitive to magnetic fluctuations entering the experimental time scale, when combining with the high temperature data, it appears that the peak in λ may be at approximately 100 K as both graphs show an increase approaching this temperature.

To make a convincing story for the critical nature calculated from the transition in both systems a brief justification of the value of T_{SP}^{μ} used within the reduced temperature plot may be worthwhile. For the fluoro sample, this is easily estimated as it is essentially a the value of a maximum of a peak in λ . Although this is an estimate, we feel that it is sound and is a value taken between two different sets of data where the values of λ both increase and look to converge at 100 K. With respect to the protio samples, the

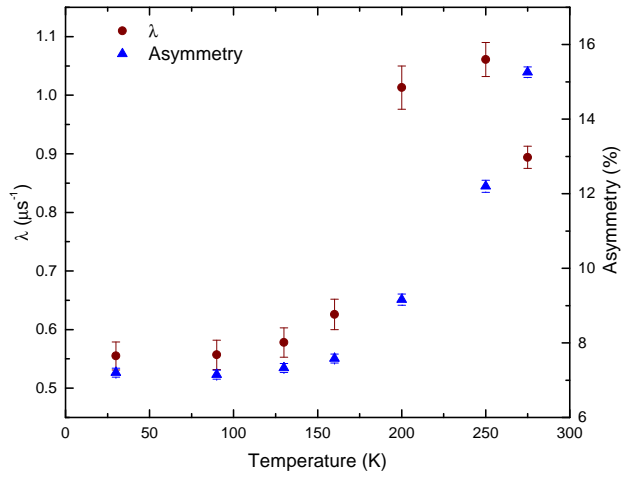


Figure 5: Low temperature muon spin relaxation rate and asymmetry for KTCNQ-H₄.

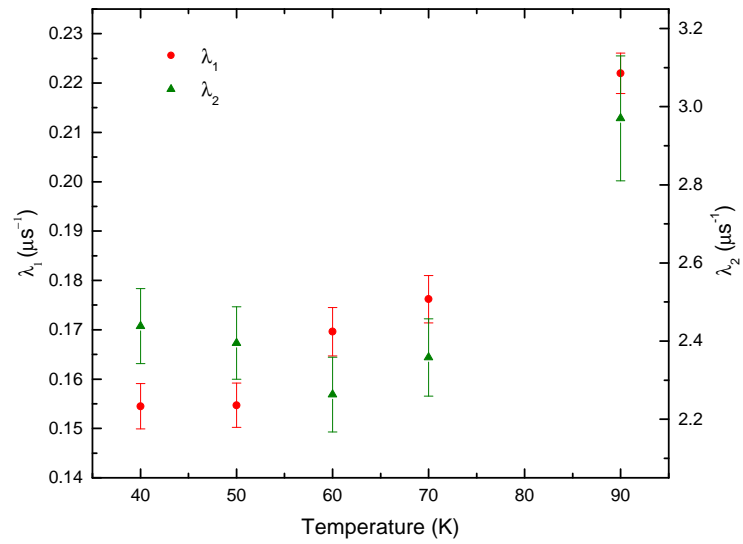


Figure 6: The muon relaxation (λ_n) at low temperature modelled using a summation of two exponentials instead of a stretched exponential for KTCNQ-F₄.

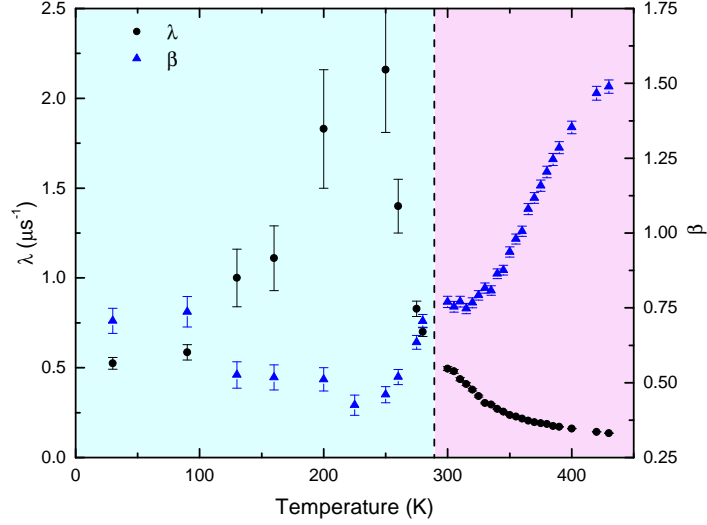


Figure 7: Muon spin relaxation and line-shape parameter for the KTCNQ-H₄ sample when analysed throughout the entire temperature range using a stretched exponential. Below 300 K the behaviour is slightly anomalous, possibly due to the bad fit of the data, but also because the relaxation may be due to a different mechanism other than simply being in a quasi-static state.

behaviour is more complex. Figure 7 shows the muon spin relaxation and line-shape parameter (β) when a stretched exponential is used to analyse the entire temperature region, from 30 to 420 K. There seem to be two distinct regions as shown on the graph where there is a clear difference in the data. The low temperature relaxation may be due to a different mechanism such as magnetism from static defects, muon mobility within the sample or even muonium formation from potassium iodide impurities. Unfortunately, getting to the bottom of this may prove to be extremely difficult or impossible. Therefore we have taken T_{SP}^μ as the value where β starts to flatten out on cooling, which is approximately 325 K. This seems like a fair estimate given the data and again, it is remarkable that the critical behaviour matches with that observed in the fluoro sample.

References

- [1] M. Konno, T. Ishii and Y. Saito. *Acta Cryst.* **B33** (1977) 763
- [2] Y. Lépine, A. Caillé and V. Larochole. *Phys. Rev. B.* **18** (1978) 3585
- [3] J. G. Vegter, T. Hibma and J. Kommandeur. *Chem. Phys. Lett.* **3** (1969) 427
- [4] A. Berlie. *PhD Thesis.* (2013) Durham University, UK
- [5] F. L. Pratt, S. J. Blundell, Th. Jestadt, B. W. Lovett, R. M. Macrae and W. Hayes. *Magn. Reson. Chem.* **38** (2000) S27
- [6] Introductory Muon Science. K. Nagamine. (2003) *Cambridge University Press, UK*
- [7] K. Nishiyama, Y. Morozumi, T. Suzuki and K. Nagamine. *Phys. Letts.* **111** (1985) 369